Coupled Systems Mechanics, *Vol. 13, No. 4 (2024) 337-357*
https://doi.org/10.12989/csm.2024.13.4.337

Nonlinear thermal vibration of fluid infiltrated magneto piezo electric variable nonlocal FG nanobeam with voids

L. Rubine[1], R. Selvamani*[1] and F. Ebrahimi[2]

[1]*Department of Mathematics, Karunya Institute of Technology and Sciences, Coimbatore-641114, Tamilnadu, India*
[2]*Department of Mechanical Engineering, Imam Khomieni International University, Qazvin, Iran*

(Received March 23, 2024, Revised June 28, 2024, Accepted July 8, 2024)

Abstract. This paper studies, the analysis of nonlinear thermal vibration of fluid-infiltrated FG nanobeam with voids. The effect of nonlinear thermal in a FG ceramic-metal nanobeam is determined using Murnaghan's model. Here the influence of fluids in the pores is investigated using the Skempton coefficient. Hamilton's principle is used to find the equation of motion of functionally graded nanobeam with the effect of refined higher-order state space strain gradient theory (SSSGT). Numerical solutions of the FG nanobeam are employed using Navier's solution. These solutions are validated against the impact of various parameters, including imperfection ratio, fluid viscosity, fluid velocity, amplitude, and piezoelectric strain, on the behavior of the fluid-infiltrated porous FG nanobeam.

Keywords: FG porous piezoelectric beam; fluid infiltrated nanobeam; nonlinear thermal; Refined higher order SSSGT; variable nonlocal

1. Introduction

A class of Japanese scientists initiated the development of Functionally Graded Materials (FGMs) as a type of composite to regulate the volume fractions of two or more materials in the mixture. These materials exhibit spatially varying properties, typically combining the best features of ceramics and metals, which makes them highly desirable in various engineering fields such as aerospace, mechanical, and biomedical engineering. The mechanical properties of FGMs, particularly their behavior under different loading conditions, have garnered significant interest among researchers. Due to their layered structure, understanding how flaws during production affect their mechanical behavior has become one of the essential objectives in contact mechanics. Ke *et al.* (2012), explores the nonlinear vibration behavior of piezoelectric nanobeams using nonlocal and Timoshenko theory. It examines the effects of size parameter, alterations in temperature and ambient electric effect of the nanobeam Ke *et al.* (2012), employed the nonlocal theory to explore the free vibration and thermo electro coupling effect of electro elastic nanobeam. Additionally, Ebrahimi *et al.* (2021), presented a study on wave scattering in viscoelastic

*Corresponding author, Ph.D., E-mail: selvam1729@gmail.com

http://www.techno-press.org/?journal=csm&subpage=8 ISSN: 2234-2184 (Print), 2234-2192 (Online)

functionally graded (FG) nano beams. Furthermore, within the context of shear bending in third mode deformation theory, vibration features of magneto thermo electro elastic FG nanobeams were studied by Ebrahimi *et al.* (2018), A new higher-order shear deformation theory for the analysis of buckling and free vibration in isotropic and functionally graded (FG) sandwich beams was put forth by the author Nguyen *et al.* (2015). Alibeigi *et al.* (2018), introduced the buckling behavior of nanobeams using the Euler-Bernoulli beam model with the inclusion of von Kármán geometrical nonlinearity. Furthermore, Shariati *et al.* (2020), investigated the bending of size dependent magneto-electro-elastic (MEE) nanobeams over nonlinear substrate. Some studies of Ebrahimi *et al.* (2020), have been carried out encompassing diverse facets. These include studies on loading of hygrothermal and bending of electromagnetically responsive piezoelectric nanobeam systems, progressive analysis of intelligent nanostructures, and frequency assessment of functionally graded thin beams after thermal post-buckling was studied by Li *et al.* Additionally, the distinction elastic nanobeams driven by stress and strain has been addressed through integral elasticity in the studies of Roamno *et al.*

A study by Barretta *et al.* employed the kinematic model to investigate buckling in beams composed of FG materials subjected to multiple thermal loads. The work of Kiani *et al.* focused on analyzing the propagation of waves in infinite functionally graded plates within a thermal environment. (Sun *et al.*, Thai *et al.*) developed a consistent refined higher-order shear deformation theory (HSDT) to examine the free vibration of functionally graded plates resting on an elastic foundation and to explore the impact of boundary conditions on natural frequencies. Thai *et al.* studied nonlinear bending in nanobeams and discussed using the (FEM) finite element method. A study by Reddy *et al.* surveyed the variation of natural frequencies using the nonlocal theory on a viscoelastic sheet. Analyzing size-dependent elements of beams was an objective of the research by Ebrahimi *et al.* Graphene sheets were used to model thermo-elastic problems in Lim *et al.* study via nonlocal strain gradient theory (NSGT). Li *et al.* examined the stiffness-softening-hardening effect of FG beams. Furthermore, Ebrahimi *et al.* discussed the free vibration of 3D FGM Euler-Bernoulli nano beams, taking into account the small-scale effect. Alibeigi *et al.* investigated the buckling response of a nanobeam was investigated by applying the Euler-Bernoulli theory (EBT) via shear models.

Another study by Ke *et al.* (2014), explored the Timoshenko beam theory to examine reliable temperature rise, external electric and magnetic potential, incorporating nonlocal formulations for magneto-electro-elastic vibrations. This analysis considered different thermal loads, as well as the influence of electrical and magnetic fields. Additionally, the bending characteristics of magneto-electro-elastic nanobeams were thoroughly investigated by Ebrahimi *et al.* (2021). Notably, studies on size-dependent advancement and issues have been employed with different shear model was studied by Ebrahimi *et al.* (2020). Additionally, Ebrahimi *et al.* (2018) delved into examine the influence of scale oriented wave propagation in different physical moduli. Notably, Ebrahimi *et al.* (2016), undertakes the investigation of hygrothermal wave characteristics in nanobeams crafted from inhomogeneous material with porosity and magnetic field. The free vibration of functionally graded doubly curved nanoshells was studied and presented findings on the vibration of FG sandwich nanoplates by Vinh *et al.* (2022). The authors Ebrahimi *et al.* (2020), discussed about the buckling behavior of MEE-FG beam with porosity phases. Temperature dependent FG beams with porosities are investigated and discussed by Ebrahimi *et al.* The stability analysis of hygrothermal environment under nonlinear thermal field was studied by Subrat *et al.* (2020). In reference with the authors Arshid *et al.* (2023), the advanced fluid infiltrated porous shells with GPLs-reinforced nanocomposite been studied with its buckling behavior. Additionally elastic buckling behavior of fluid infiltrated porous plates with an analytical approach was studied by Rad *et al.* (2020). The authors Selvamani *et al.* (2023), discussed about the vibration analysis of magneto thermo piezoelectric functionally graded material (FGM) nanobeam. In a reference which describes the two entirely different physical characteristics of materials and structures at nanoscale by Lim *et al.* (2015). In Ghobadi *et al.* (2020) studied the size-dependent nonlinear free vibration of functionally graded flexoelectric nano-plate under the magnetic field. Alghamdi *et al.* (2024) investigated the vibration of a thermoelastic nano-ceramic (Si3N4) beam exposed to a magnetic field under the effect of a moving heat source and different types of thermal loads. The torsional porous flexoelectric microtubes made of functionally graded (FG) materials are investigated by Beni *et al.* (2022). Mirjavadi *et al.* (2020) nonlinear dynamic characteristics of a nonlocal two-phase piezo-magnetic beam including geometric imperfections by considering piezoelectric reinforcement scheme. Beni *et al.* (2022) analyzed the dynamic stability of an isotropic viscoelastic Euler-Bernoulli nano-beam using piezoelectric materials. Wave propagation analysis of a FG nanobeam with rectangular cross section resting on Visco-Pasternak foundation was studied by Arefi *et al.* (2017). Author Beni *et al.* (2023) studied the electro-thermal buckling in a flexoelectric microbeam. Flexoelectric/piezoelectric in a rotating microbeams was studied by the author Hosseini *et al.* (2023). Authors Wan *et al.* (2019) nonlinear thermal buckling and post-buckling of magneto-electro-thermo-elastic functionally graded porous nanobeams is analyzed. Despite, these significant contributions, there remains a need for a comprehensive study that considers the combined effects of nonlinear thermal vibrations, fluid infiltration, and the interaction of magnetic and piezoelectric fields on FG nanobeams with voids. This paper builds upon these foundational studies by focusing on the nonlinear thermal vibration behavior of fluid-infiltrated magneto-piezoelectric variable nonlocal FG nanobeams with voids. Nonlinear thermal effects can significantly alter the stiffness and damping characteristics of nanobeams, impacting their stability and functionality. The presence of voids and fluid infiltration further complicates the vibrational response, influencing the material's overall performance. By considering the interactions between thermal, electrical, and magnetic fields, along with the effects of fluid infiltration and structural imperfections, this study aims to provide a comprehensive analysis of these complex systems. The novelty of this work is to understand the interplay of multiple physical phenomena in FG nanobeams, which is critical for designing advanced materials capable of operating effectively under combined thermal, electrical, and magnetic conditions.

The objective of this study is to explore the effects of nonlinear thermal vibration on a fluid-infiltrated porous nanobeam, taking into account nonlocal variables. The structure of this paper is outlined as follows: Section 2 establishes the fundamental equations governing the behavior of the fluid-infiltrated porous FG nanobeam under nonlinear thermal conditions. In Section 3, the equations of motion considering the nonlocal nature of the FG nanobeam are derived based on Hamilton's principle. Section 4 employs Navier's solution technique to solve the motion equations. Finally, a summary of the conclusions along with graphical results is presented.

2. Formulation of the problem

An examination of thermo-electro-magneto functionally graded material (FGM) has been followed up using the refined higher order SSSGT. The nanobeam possesses dimensions including length (L), width $(b)$and thickness $(\hat{h})$. The FGM, in this case, is comprised of two distinct sections: a ceramic segment $\mathrm{BaTiO_3}$ and a metallic segment CoFe_2O_4. In order to accommodate behaviors influenced by temperature, the study incorporates an analysis of the individual components within the FGM.

In this section, the properties have been computed using power-law relations. To determine these properties in the thickness direction with respect to temperature variable, the volume fraction of metallic and ceramic phase is calculated using the power law model. Consequently, the fractional volume of the ceramic part can be Ebrahimi (2021)

$$F_c = \left(\frac{z}{\hat{h}} + \frac{1}{2}\right)^p, F_m + F_c = 1 \tag{2.1}$$

While the exponential power law p and thickness $\hat{h}$ explore the property distributions in each layer of the nanobeam and the desired material property can be considered at local temperature as (Ebrahimi 2021)

$$P = P_0(P_{-1}T^{-1} + 1 + P_1T + P_2T^2 + P_3T^3) \tag{2.2}$$

whereas, $P_0, P_{-1}, P_1, P_2, P_3$ are the coefficients of material phases.

2.1 Porous MPE (Magneto Piezo Electric) FG nanobeam

The effective material properties P_f of FGM nanobeam by using the modified rule of mixture can be expressed by Arshid *et al.* (2023)

$$P_f = P_m(F_m - \frac{\alpha}{2}) + P_c(F_c - \frac{\alpha}{2}) \tag{2.3}$$

Here, P_m and F_m is the metal property and volume fraction of metallic property. P_c and F_c is the ceramic property and its volume fraction. According to the Eqs. (2.1) and (2.3) the effective material properties of porous MPE nanobeam with even porosities across the thickness direction is

$$P(z) = (P_c - P_m)\left(\frac{z}{\hat{h}} + \frac{1}{2}\right)^p + P_m - (P_c + P_m)\frac{\alpha}{2} \tag{2.4}$$

2.2 Kinematic relations

Eringen's theory of nonlocality proposes that the stress state at a particular location within a body is a function of the strains across all adjacent regions. The fundamental equations for this theory, considering the absence of body related forces, can be expressed in the following manner: Xiao *et al.* (2019)

$$\begin{gathered}
\sigma_{ij} = \int_v \alpha(|y'' - y'|, \tau)[C'_{ijkl}\varepsilon_{kl}(y'') - e_{mij}E_m(y'') - \Omega_n(y'') - C'_{ijkl}\alpha_{kl}\Delta T]dV(y'') \\
D_i = \int_v \alpha(|y'' - y'|, \tau)[e_{ikl}\varepsilon_{kl}(y'') - E_m(y'') + \Omega_n(y'') - \Delta T]dV(y'') \\
B_i = \int_v \alpha(|y'' - y'|, \tau)[\varepsilon_{kl}(y'') + E_m(x') + \chi_{ni}\Omega_n(y'') - \lambda_i\Delta T]dV(y'')
\end{gathered} \tag{2.5}$$

Here, the symbols σ_{ij} and ε_{ij} represents stress and strain. E_i and D_i denotes electric field and electric displacement, while B_i indicates magnetic induction and Ω_i as magnetic field. The terms α_{kl} and ΔT encompass thermal variation moduli and temperature difference. Furthermore, C'_{ijkl}

and e_{mij} represents the elastic and piezoelectric terms. Whereas, magnetic constant is denoted as χ_{ij}. Additionally, $\tau = e_0 a/l$ defines the scale coefficient and as well asa, lstand for characteristic lengths within the internal and external facets, respectively. e_0 is constant of the material considered.

The governing equations of the nanobeam are derived using a precise kinematic theory that accounts for accurate stress-strain variations in rigid materials. Additionally, the higher-order shear deformation theory provides insight into these stress-strain changes. Based on Ebrahimi (2021), we consider the refined deformable shear beam's direction as

$$u_x(x,z,\tilde{t}) = u(x,\tilde{t}) - \frac{\partial w_b(x,\tilde{t})}{\partial x} z - \frac{\partial w_s(x,\tilde{t})}{\partial x} \Upsilon(z) \tag{2.6}$$

$$w_z(x,z,\tilde{t}) = w_b(x,\tilde{t}) + w_s(x,\tilde{t}) \tag{2.7}$$

Here, u, w_b and w_s are the longitudinal, bending and shear components of the transverse displacement. Furthermore, with the intention of shear strain dispersion, $\Upsilon(z)$ is the interpolation function (shape function) which is designed as Ebrahimi (2021)

$$\Upsilon(z) = \frac{\hat{h} e^z}{\hat{h}^2 + \pi^2}\left[\pi \sin\left(\frac{\pi z}{\hat{h}}\right) + \hat{h} \cos\left(\frac{\pi z}{\hat{h}}\right)\right] - \frac{\hat{h}^2}{\hat{h}^2 + \pi^2} \tag{2.8}$$

When addressing the presence of shear strain and stress within the deformed structural cross-section through this function, uncertainties arise. Nevertheless, it is imperative to maintain the assumption of shear strain absence at free surfaces. The nonzero strains can be described using the continuum infinitesimal strain tensor.

$$\varepsilon_{xx} = \frac{\partial u}{\partial x} - z\frac{\partial^2 w_b}{\partial x^2} - \Upsilon(z)\frac{\partial^2 w_s}{\partial x^2} \tag{2.9}$$

$$\gamma_{xz} = \Gamma(z)\frac{\partial w_s}{\partial x} \tag{2.10}$$

As

$$\Gamma(z) = 1 - \frac{d\Upsilon(z)}{dz} \tag{2.11}$$

In matrix form

$$\{\varepsilon_{xx}\} = \{\varepsilon_{xx}^0\} + z\{\varepsilon_{xx}^1\} + \Upsilon(z)\{\varepsilon_{xx}^2\} \tag{2.12}$$

$$\{\gamma_{xz}\} = \Gamma(z)\{\gamma_{xz}^0\} \tag{2.13}$$

In which

$$\begin{gathered}
\{\varepsilon_{xx}^0\} = \left\{\frac{\partial u}{\partial x}\right\} \\
\{\varepsilon_{xx}^1\} = -\left\{\frac{\partial^2 w_b}{\partial x^2}\right\} \\
\{\varepsilon_{xx}^2\} = \left\{\frac{\partial w_s}{\partial x}\right\} \\
\{\gamma_{xz}^0\} = \{w_s\}
\end{gathered} \tag{2.14}$$

2.3 Constitutive relations

The constitutive relation of the nanobeam is, Vinh and Tounsi (2022)

$$\begin{Bmatrix}\sigma_{xx}\\ \tau_{xz}\end{Bmatrix} = \begin{Bmatrix}c_{11} & 0\\ 0 & c_{66}\end{Bmatrix}\begin{Bmatrix}\varepsilon_{xx}\\ \gamma_{xz}\end{Bmatrix} \tag{2.15}$$

Such as, $c_{11} = \frac{E(z)}{1-\nu^2}$; $c_{66} = \frac{E(z)}{2(1+\nu)}$

2.4 Review of nonlinear thermal environment

Based on thermal elasticity theory, the axial force due to thermal environment (N_T) can be given as, Subrat Kumar Jen *et al. (*2020)

$$N_T = \int_{-h/2}^{h/2} (c_{11}(z), c_{66}(z))\alpha_x(z)\Psi(\Delta T)dz \tag{2.16}$$

In which $\Psi(\Delta T)$ is the nonlinear elastic stress temperature coefficient which may be defined as

$$\Psi(\Delta T) = E\alpha_x \Delta T - \hat{h}\alpha_x^2 \Delta T^2 \tag{2.17}$$

with $\hat{h} = l_1(1-2\nu) - 2m_1(\nu^2 - 1) + n_1\nu^2$

where ΔT is the change in temperature, α_x is the coefficient of thermal expansion, (l_1, m_1, n_1) are Murnaghan's third order elastic constants and ν is the Poisson's ratio. Substituting the above equations

$$\begin{aligned} N_T &= \int_A \Psi(\Delta T)dA \\ &= \int_A (E\alpha_x \Delta T - \hat{h}\alpha_x^2 \Delta T^2)dA \\ &= EA\alpha_x \Delta T - A\hat{h}\alpha_x^2 \Delta T^2 \end{aligned} \tag{2.18}$$

2.5 Fluid infiltrated MPE porous FG nanobeam

Here, the MEPT FG nanobeam porous core is infiltrated with fluid and the stiffness components for the fluid can be stated in two terms namely, drained (ν) and undrained (ν_u) Poisson's ratio, Arshid *et al.* (2023)

$$c_{11} = 2G(z)\frac{1-4\nu+2\nu_u}{1-3\nu+2\nu\nu_u} \tag{2.19}$$

$$c_{66} = 2G(z)\frac{-\nu+2(1-\nu)\nu_u}{1-3\nu+2\nu\nu_u} \tag{2.20}$$

Where, $\nu_u = \frac{(3\nu+\Delta)}{(3-\Delta)}$,

In which $\Delta = B\lambda(z)(1-2\nu)$; where the Skempton coefficient is depicted by B that demonstrates the pressure of the fluid inside the pores, $\lambda(z)$ is the Biot's coefficient that can be determined via $1 - G(z)/G_0$. Also $G(z)$ equals $E(z)/2(1+\nu).E(z)$ is Young's elasticity modulus of the nanobeam. The material properties of the FG nanobeam can be

$$\begin{Bmatrix} E(z) \\ \rho(z) \\ \alpha_x(z) \end{Bmatrix} = \begin{Bmatrix} E_1 \\ \rho_1 \\ \alpha_1 \end{Bmatrix} \left(1 - \begin{Bmatrix} \theta \\ 1-\sqrt{1-\theta} \\ 1-\sqrt{1-\theta} \end{Bmatrix} \Re(z) \right) \tag{2.21}$$

Here, θ is the imperfection ratio which is demarcated as the ratio of pores to the whole volume. $\Re(z)$ is the imperfection function. And the three distinguished types of imperfection are Arshid *et al. (*2023),

Imperfection type 1:

If the pores are scattered non-symmetrically then

$$\Re(z) = cos\left[\frac{\pi}{2\hat{h}}\left(z + \frac{\hat{h}}{2}\right)\right] \tag{2.22}$$

Imperfection type 2:

$$\Re(z) = cos\left(\frac{\pi z}{\hat{h}}\right) \tag{2.23}$$

Imperfection type 3:

If the pores are thickness free then this pattern rules for Young's modulus and density

$$\begin{aligned} E(z) &= E_1(1-\theta\chi) \\ \rho(z) &= \rho_1\sqrt{1-\theta\chi} \\ \alpha_x(z) &= \alpha_1\sqrt{1-\theta\chi} \end{aligned} \tag{2.24}$$

Where

$$\chi = \frac{1}{\theta} - \frac{1}{\theta}\left(\frac{2}{\pi}\sqrt{1-\theta} - \frac{2}{\pi} + 1\right)^2 \tag{2.25}$$

2.6 Nonlocal elasticity theory

The concept of nonlocal elasticity theory postulates that the stress experienced at any point is impacted by the strains occurring at all neighboring points within the continuum body. The nonlocal parameter remains constant irrespective of variation of materials. The differential form of the nonlocal elastic theory is as follows

$$(1-\mu\nabla^2)\sigma_{ij} = \xi_{ij} \tag{2.26}$$

Where σ_{ij}, ξ_{ij} are nonlocal stress and stress tensors, $\nabla^2 = \frac{\partial^2}{\partial x^2} + \frac{\partial^2}{\partial y^2}$ is the second Laplace operator, $\mu = (e_0 a)^2$ is the nonlocal parameter, e_0 is a material constant and a is an internal characteristic length. In this study, it is postulated that the nonlocal parameter undergoes alteration concurrent with the modifications in other material attributes within the functionally graded material Vinh and Tounsi (2022).

$$\begin{aligned} \begin{Bmatrix} \xi_{xx} \\ \xi_{xz} \end{Bmatrix} &= \begin{Bmatrix} \sigma_{xx} \\ \tau_{xz} \end{Bmatrix} - \mu(z)\nabla^2 \begin{Bmatrix} \sigma_{xx} \\ \tau_{xz} \end{Bmatrix} \\ &= \begin{bmatrix} c_{11} & 0 \\ 0 & c_{55} \end{bmatrix} \begin{Bmatrix} \varepsilon_{xx} \\ \gamma_{xz} \end{Bmatrix} \end{aligned} \tag{2.27}$$

The influence of the nonlocal parameter varies along the thickness dimension of the functionally graded nanobeam. The connection between nonlocal stress and strain is not solely governed by changes in Young's modulus and Poisson's ratio; it also hinges on variations in the nonlocal parameter.

3. Motion equations

The protracted lagrangian can be defined in accordance with Hamilton's principle is

$$L = T - K + H$$

Therefore, Hamilton's principle can be expressed as

$$\delta \int_{\tilde{t}_1}^{\tilde{t}_2} (T - K + H) d\tilde{t} = 0 \tag{3.1}$$

In Eq. (3.1), variables Tstrain energy, H work done and K is the kinetic energy. Hence, the virtual strain energy can be

$$\delta T = \int_0^L (\sigma_{xx}\delta\varepsilon_{xx} + \tau_{xz}\delta\gamma_{xz} - D_x\delta E_x - D_z\delta E_z)dx \tag{3.2}$$

$$\phi(x,z,\tilde{t}) = -\cos(\beta z)\,\phi(x,\tilde{t}) + \frac{2zV_0}{\hat{h}} e^{-ik\tilde{t}} \tag{3.3}$$

Where, $D_z = e_{31}\varepsilon_{xx} + e_{33}E_z$ and $D_x = e_{15}\gamma_{xz} + e_{11}E_x$. The variation of electric potential towards the direction of x is $\beta = \pi/\hat{h}; \phi(x,\tilde{t})$; Ω is the natural frequency of the piezoelectric nanobeam and V_0 is the external electric voltage.

By infusing Eqs. (2.9) and (2.10) in Eq. (3.2)

$$\delta T = \int_0^L \left(N\frac{\partial \delta u}{\partial x} - M_b \frac{\partial^2 \delta w_b}{\partial x^2} - M_s \frac{\partial^2 \delta w_s}{\partial x^2} + Q\frac{\partial \delta w_b}{\partial x} - D_x E_x - D_z E_z \right) dx \tag{3.4}$$

the stress resultants can be obtained

$$[N, M_b, M_s] = \int_A [1, z, \Upsilon(z)]\sigma_{xx} dA \tag{3.5}$$

$$Q = \int_A \Gamma(z)\sigma_{xz} dA \tag{3.6}$$

The kinetic energy of the system can be arrived as

$$\delta K = \int_0^L \rho(z) \left[\frac{\partial u_x}{\partial \tilde{t}} \frac{\partial \delta u_x}{\partial \tilde{t}} + \frac{\partial u_z}{\partial \tilde{t}} \frac{\partial \delta u_z}{\partial \tilde{t}} \right] dx \tag{3.7}$$

Infusion of Eqs. (2.6) and (2.7) in the Eq. (3.7)

$$\delta K=\int_0^L\left(\begin{array}{c} I_0^*\left(\frac{\partial u}{\partial\tilde{t}}\frac{\partial\delta u}{\partial\tilde{t}}+\frac{\partial(w_b+w_s)}{\partial\tilde{t}}\frac{\partial\delta(w_b+w_s)}{\partial\tilde{t}}\right)\\ -I_1^*\left(\frac{\partial u}{\partial\tilde{t}}\frac{\partial^2\delta w_b}{\partial x\,\partial\tilde{t}}+\frac{\partial^2 w_b}{\partial x\,\partial\tilde{t}}\frac{\partial\delta u}{\partial\tilde{t}}\right)\\ -J_1^*\left(\frac{\partial u}{\partial\tilde{t}}\frac{\partial^2\delta w_s}{\partial x\,\partial\tilde{t}}+\frac{\partial^2 w_s}{\partial x\,\partial\tilde{t}}\frac{\partial\delta u}{\partial\tilde{t}}\right)\\ +I_2^*\frac{\partial^2 w_b}{\partial x\,\partial\tilde{t}}\frac{\partial^2\delta w_b}{\partial x\,\partial\tilde{t}}+K_2^*\frac{\partial^2 w_s}{\partial x\,\partial\tilde{t}}\frac{\partial^2\delta w_s}{\partial x\,\partial\tilde{t}}\\ +J_2^*\left(\frac{\partial^2 w_b}{\partial x\,\partial\tilde{t}}\frac{\partial^2\delta w_s}{\partial x\,\partial\tilde{t}}+\frac{\partial^2 w_s}{\partial x\,\partial\tilde{t}}\frac{\partial^2\delta w_b}{\partial x\,\partial\tilde{t}}\right)\end{array}\right)dx \tag{3.8}$$

In accordance with the magnetic field

$$M_B=\eta A\Omega_x^2\frac{\partial^2 w}{\partial x^2}$$

Whereas, M_B is magnetic field; η is field permeability; A is cross sectional area of the nanobeam and Ω_x stands for magnetic potential of the longitudinal magnetic field, the work done N_x with a temperature fluctuation due to thermal environment can be

$$\delta H=\left(\frac{1}{2}\int_0^L N_x+EA\alpha_x\Delta T-A\hat{h}\alpha_x^2\Delta T^2+\eta\Omega_x^2\frac{\partial^2 w}{\partial x^2}\right)dx \tag{3.9}$$

Coupled Euler-Lagrange equation is derived from the Eqs. (3.4), (3.8) and (3.9) as

$$\frac{\partial N}{\partial x}=I_0^*\frac{\partial^2 u}{\partial\tilde{t}^2}-I_1^*\frac{\partial^3 w_b}{\partial x\,\partial\tilde{t}^2}-J_1^*\frac{\partial^3 w_s}{\partial x\,\partial\tilde{t}^2} \tag{3.10}$$

$$\begin{aligned}\frac{\partial^2 M_b}{\partial x^2}&=I_0^*\frac{\partial^2(w_b+w_s)}{\partial\tilde{t}^2}+I_1^*\frac{\partial^3 u}{\partial x\,\partial\tilde{t}^2}-I_2^*\frac{\partial^4 w_b}{\partial x^2\,\partial\tilde{t}^2}-J_2^*\frac{\partial^4 w_s}{\partial x^2\,\partial\tilde{t}^2}\\ &-\left(N_x+EA\alpha_x\varDelta T-A\hat{h}\alpha_x^2\varDelta T^2+\eta\varOmega_x^2\frac{\partial^2 w}{\partial x^2}\right)\end{aligned} \tag{3.11}$$

$$\begin{aligned}\frac{\partial^2 M_s}{\partial x^2}+\frac{\partial Q_{xz}}{\partial x}-N_x\frac{\partial^2 w}{\partial x^2}&=\left(I_0^*\frac{\partial^2(w_b+w_s)}{\partial\tilde{t}^2}+J_1^*\frac{\partial^3 u}{\partial x\,\partial\tilde{t}^2}-J_2^*\frac{\partial^4 w_b}{\partial x^2\,\partial\tilde{t}^2}-K_2^*\frac{\partial^4 w_s}{\partial x^2\,\partial\tilde{t}^2}\right)\\ &-\left(N_x+EA\alpha_x\varDelta T-A\hat{h}\alpha_x^2\varDelta T^2+\eta\varOmega_x^2\frac{\partial^2 w}{\partial x^2}\right)\end{aligned} \tag{3.12}$$

$$\delta\phi=\int_{\frac{-\hat{h}}{2}}^{\frac{\hat{h}}{2}}\left[\cos(\beta z)\left(\frac{\partial Dx}{\partial x}\right)\right]+\beta\sin(\beta z)\,Dz \tag{3.13}$$

Where, N, M^b, M^s and Q^{xz} are the stress resultants and calculated as

$$(N_{xx})=\int_0^L(\xi_{xx})dz$$

$$(M_{xx}^b) = \int_0^L (\xi_{xx}) z dz$$
$$(M_{xx}^s) = \int_0^L (\xi_{xx}) \Upsilon(z) dz$$
$$(Q_{xz}) = \int_0^L (\xi_{xz}) \Gamma(z) dz \tag{3.14}$$
$$(D_{xz}) = \int_0^L (\xi_{xz}) \phi(z) dz$$

Substituting (2.17) in (3.14)

$$\begin{Bmatrix} N \\ M^b \\ M^s \\ Q \end{Bmatrix} = \begin{bmatrix} A & B & 0 & 0 \\ B & D & F & 0 \\ E & F & H & 0 \\ 0 & 0 & 0 & A_s \end{bmatrix} \begin{Bmatrix} {\varepsilon_{xx}}^0 \\ {\varepsilon_{xx}}^1 \\ {\varepsilon_{xx}}^2 \\ {\gamma_{xz}}^0 \end{Bmatrix} \tag{3.15}$$

Where,

$$N = \{N_{xx}\}, M^b = \{M_{xx}^b\}, M^s = \{M_{xx}^s\}, Q = \{Q_{xz}\}$$

$$\varepsilon^0 = \{\varepsilon_{xx}^0\}, \varepsilon^1 = \{\varepsilon_{xx}^1\}, \varepsilon^2 = \{\varepsilon_{xx}^2\}, \gamma^0 = \{\gamma_{xz}^0\}$$

The inertial mass moments from the above definition can be defined as,

$$[I_0^*, I_1^*, I_2^*, J_1^*, J_2^*, K_2^*] = \int_A \mu(z)\rho(z)[1, z, z^2, \Upsilon(z), z\Upsilon(z), \Upsilon^2(z)]dx$$

The material properties considered in this analysis include the effective mass density $\rho(z)$ and effective nonlocal parameter $\mu(z)$. While the nonlocal parameter shows variations across different materials, a variable nonlocal parameter implies that nonlocal effects can vary spatially or with respect to specific parameters within the structure. This parameter adapts to the model, influenced by factors like material properties, dimensions, or environmental conditions. The parameter denoted as $\kappa = \mu_c/\mu_m$ represents the proportion between the ceramic and metal phases. In cases where the nonlocal parameter is constant, κequals one ($\kappa = 1$). Vinh and Tounsi (2022).

4. Analytical solution

In this study, the Navier's solution technique is employed to solve the equation of motion.

$$u(x, \tilde{t}) = \sum_{n=1}^{\infty} u_n \cos(\frac{n\pi}{L}) x e^{i\omega\tilde{t}}$$
$$w(x, \tilde{t}) = \sum_{n=1}^{\infty} w_n \sin(\frac{n\pi}{L}) x e^{i\omega\tilde{t}}$$
$$Q(x, \tilde{t}) = \sum_{n=1}^{\infty} Q_n \cos(\frac{n\pi}{L}) x e^{i\omega\tilde{t}}$$

$$\phi(x,\tilde{t}) = \sum_{n=1}^{\infty} \phi_n \, sin(\frac{n\pi}{L}) x e^{i\omega\tilde{t}} \tag{4.1}$$

$$\begin{Bmatrix} u \\ w_b \\ w_s \end{Bmatrix} = \begin{Bmatrix} u \, exp[i(\beta x - \Omega\tilde{t})] \\ w_b \, exp[i(\beta x - \Omega\tilde{t})] \\ w_s \, exp[i(\beta x - \Omega\tilde{t})] \end{Bmatrix} \tag{4.2}$$

The amplitudes of the propagating waves are denoted as u, w_b and w_s. Whereas, Ω is frequency and β is the wave number. And substituting the above expression into the Eqs. (3.10)-(3.13), then the attained form will be

$$\{[K_s] + [C_d]\Omega + [M_m]\Omega^2\} \begin{Bmatrix} u \\ w_b \\ w_s \end{Bmatrix} = 0 \tag{4.3}$$

From the above definition $[K_s]$ represents stiffness, $[C_d]$ stands for damping and $[M_m]$ is for mass matrices. The elements of these matrices are

$$\begin{gathered}
k_{a1}^s = (1 + \lambda^2\beta^2) A_{xx}\beta^2 \\
k_{a2}^s = i\left(N_x + \eta\Omega_x^2\right)(1 + \lambda^2\beta^2) B_{xx}\beta^5 \\
k_{a3}^s = i\left(N_x + \eta\Omega_x^2\right)(1 + \lambda^2\beta^2) B_{xx}^s\beta^5 \\
k_{a4}^s = e_{31}(1 - \lambda^2\beta^2)\beta \, sin(\beta z)\phi - \frac{2V_0 e^{ik\tilde{t}}}{\hat{h}} \\
k_{b2}^s = -\left(N_x + \eta\Omega_x^2\right) EA\alpha_x \Delta T - A\hat{h}\alpha_x^2 \Delta T^2 (1 + \lambda^2\beta^2) D_{xx}\beta^6 \\
k_{b3}^s = -\left(N_x + \eta\Omega_x^2\right) EA\alpha_x \Delta T - A\hat{h}\alpha_x^2 \Delta T^2 (1 + \lambda^2\beta^2) D_{xx}^s\beta^6 \\
k_{b4}^s = e_{31}(1 - \lambda^2\beta^2)\beta \, sin(\beta z)\phi - \frac{2V_0 e^{ik\tilde{t}}}{\hat{h}} \\
k_{c3}^s = -\left(N_x + \eta\Omega_x^2\right) EA\alpha_x \Delta T - A\hat{h}\alpha_x^2 \Delta T^2 (1 + \lambda^2\beta^2)(H_{xx}^s\beta^6 + A^s\beta^4) \\
k_{c4}^s = e_{31}(1 - \lambda^2\beta^2)\beta^2 \, sin(\beta z)\phi - \frac{2V_0 e^{ik\tilde{t}}}{\hat{h}}
\end{gathered} \tag{4.4}$$

$$\begin{gathered}
c_{a1}^d = -A_{xx}\tau\beta^2 \\
c_{a2}^d = i\left(N_x + \eta\Omega_x^2\right) B_{xx}\tau\beta^5 \\
c_{a3}^d = i\left(N_x + \eta\Omega_x^2\right) B_{xx}^s\tau\beta^5 \\
c_{a4}^d = \tau e_{31}\left(\beta^2 \cos(\beta z)\frac{dz}{dt}\phi - \left(\frac{2V_0 e^{ik\tilde{t}}}{\hat{h}}(ik)\right)\right) \\
c_{b2}^d = -\left(N_x + \eta\Omega_x^2\right) D_{xx}\tau\beta^6 \\
c_{b3}^d = -\left(N_x + \eta\Omega_x^2\right) D_{xx}^s\tau\beta^6 \\
c_{b4}^d = \tau e_{31}\left(\beta^2 \cos(\beta z)\frac{dz}{dt}\phi - \left(\frac{2V_0 e^{ik\tilde{t}}}{\hat{h}}(ik)\right)\right) \\
c_{c3}^d = -\left(N_x + \eta\Omega_x^2\right)\tau\beta^4 (H_{xx}^s\beta^2 + A_s)
\end{gathered}$$

$$c_{c4}^{d} = \tau e_{31}\left(\beta^2 cos(\beta z)\frac{dz}{dt}\phi - \left(\frac{2V_0 e^{ik\tilde{t}}}{\hat{h}}(ik)\right)\right) \quad (4.5)$$

$$\begin{gathered} m_{a1}^{m} = -(1+\mu(z)^2\beta^2)I_0^* \\ m_{a2}^{m} = i\left(N_x+\eta\Omega_x^2\right)\beta^2(1+\mu(z)^2\beta^2)I_1^* \\ m_{a3}^{m} = i\left(N_x+\eta\Omega_x^2\right)\beta^2(1+\mu(z)^2\beta^2)J_1^* \\ m_{b2}^{m} = -(1+\mu(z)^2\beta^2)\left(I_0^*+I_2^*\left(N_x+\eta\Omega_x^2\right)\beta^4\right) \\ m_{b3}^{m} = -(1+\mu(z)^2\beta^2)(I_0^*+J_2^*\left(N_x+\eta\Omega_x^2\right)\beta^4) \\ m_{c3}^{m} = -(1+\mu(z)^2\beta^2)\left(I_0^*+K_2^*\left(N_x+\eta\Omega_x^2\right)\beta^2\right) \\ m_{c4}^{m} = (1+\mu(z)^2\beta^2)e_{31}\left(\beta^2 cos(\beta z)\frac{dz}{dt}\phi - \left(\frac{2V_0 e^{ik\tilde{t}}}{\hat{h}}(ik)\right)\right) \end{gathered} \quad (4.6)$$

5. Results and discussion

This section illustrates the magneto-thermo vibration of FG Nanobeam with the numerical examples. Table 1 presents the material properties of $BaTiO_3$, $CoFe_2O_4$ while Table 2 details the material properties related to piezoelectricity PZT-4. Table 3 provides a comparison of the non-dimensional critical buckling load of the FGM beam for various power-law exponent values by taking the nonlocal parameter as $\mu_c = \mu_m = 0$, without fluid environment. From Table 3, we can see a consistent agreement of the physical varibles with the literature, Nguyen *et al. (*2015).

Fig. 1 illustrates the influence of nonlocal values on varying temperature gradient and imperfection ratio. For materials with weaker nonlocal effects ($e_0 = 1$), the temperature gradient may exhibit a moderate increase or remain relatively stable with increasing imperfection ratio. Conversely, materials with stronger nonlocal effects ($e_0 = 1.5$ or 2) may show a more pronounced decrease in temperature gradient as the imperfection ratio increases. Fig. 2 illustrates the impact of imperfection ratio on the nondimensional frequency via different nonlocal parameters, specifically characterized by different values of e_0. The imperfection ratio shows a decreasing trend with developing nonlocal material constants e_0 from 1 to 2 as the nondimensional frequency increases.

The variation of magnetic potential to wave frequency with full ceramic shows an increase in natural frequency with the magnetic potential. Additionally, it is noted that when the material is ceramic-rich ($\mu_c = 0.1$ to 0.4), then the magnetic potential increases with an increase in the

Table 1 Material properties of $BaTiO_3$ and $CoFe_2O_4$

Material	Properties			
$BaTiO_3$	E [Pa]	166	e_{33} (N/m^{2}K)	(7.124×10^{-9})
	ρ [kg/m^3]	5800	e_{15} (c/m^2)	14.1
	ν [-]	1.1945		
$CoFe_2O_4$	E [Pa]	286	e_{31} (c/m^2)	-(4.1)
	ρ [kg/m^3]	5300	e_{11} (c/Vm)	(5.841×10^{-9})
	ν [-]	1.167		

Table 2 Material property of PZT-4, Ke *et al.* (2012)

PZT - 4	e_{31} (c/m^2)	e_{11} (c/Vm)	e_{33} (N/m^{2}K)	e_{15} (c/m^2)
	-4.1	5.841×10^{-9}	7.124×10^{-9}	14.1

Table 3 Comparison of non-dimensional critical buckling load of FGM beam for various power-law exponents, Nguyen *et al.* (2015)

L/h		*p*=0	*p*=0.5	*p*=1	*p*=2	*p*=5	*p*=10
5	(Nguyen *et al.* 2015)	48.8406	32.0013	24.6894	19.1577	15.7355	14.1448
	Present	48.835	31.967	24.6870	19.1605	15.7401	14.13
10	(Nguyen *et al.* 2015)	52.3083	34.0002	26.1707	20.3909	17.1091	15.5278
	Present	52.3082	34.0087	26.1727	20.3936	17.1118	15.5291

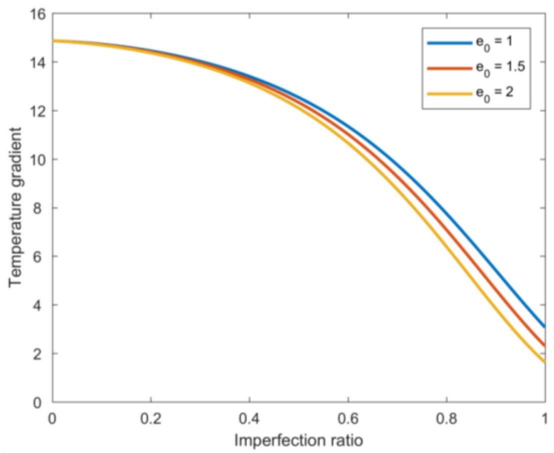

Fig. 1 Influence of nonlocality on temperature gradient and imperfection ratio

natural frequency $\Omega = 0.5$ as shown in Fig. 3. Similarly, Fig. 4 shows that the frequency and magnetic potential increase with an increase in the metallic-rich nonlocal variable from ($\mu_m = 0.1$ to 0.4) . In Fig. 5, the changes in dimensionless frequency against fluid velocity is presented, it is seen that the convergence occurs until a specific point, beyond which resonance phenomena are initiated among the modes. When the dimensionless frequency converges till the fluid velocity reaches 3.0, resonance behavior occurs with higher fluid velocity. Also, damping occurs when the fluid velocity reaches 4.4 along with increasing dimensionless frequencies in the context of metallic nonlocal variable.

Applications in microfluidic sensors demonstrate that higher fluid viscosity decreases the dimensionless frequency, indicating that more viscous fluids dampen the vibrations of the FG nanobeam, leading to a slower response, while higher fluid velocity induces a resonant behavior with the dimensionless frequency, suggesting that increased fluid flow can amplify the vibrations, potentially enhancing the dynamic response of the nanobeam. In Fig. 6, a gradual decrease in honey's behavior is observed, starting around 1.2 and damping at 1.0, exhibiting a resonant response driven by the influence of the nonlocal metal variable at smaller scales. In comparison, water, with its inherently lower viscosity, demonstrates less damping and a milder response to the nonlocal metal variable at smaller scales than honey. Furthermore, when contrasted with honey

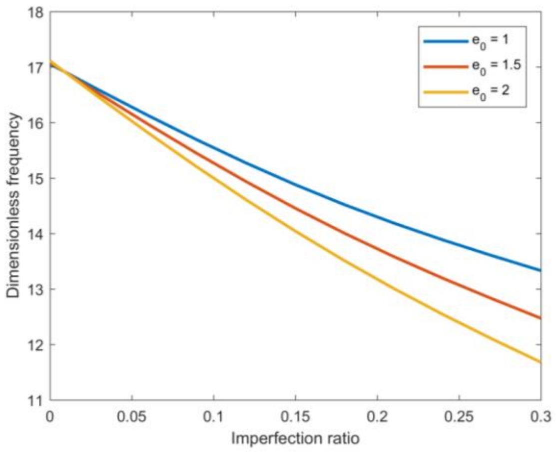

Fig. 2 Influence of nonlocality on dimensionless frequency and imperfection ratio

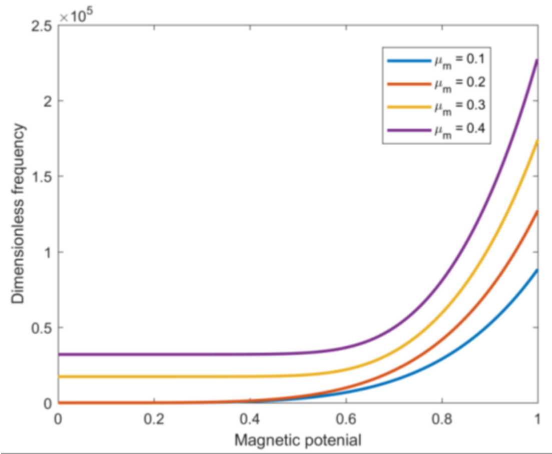

Fig. 3 The variation of dimensionless frequency versus magnetic potential with the dominance of metal phase

and water, vacuum responds more favorably to the dynamic interaction of dimensionless frequency and fluid viscosity. Similarly, in Fig. 7, the variation of dimensionless frequency over fluid viscosity in the context of ceramic nonlocal variable has been studied. Comparing honey and water, honey shows a damping behavior, potentially influenced by ceramic nonlocal variable, whereas water shows a moderate damping behavior. Hence, honey, water, and vacuum converge at some point.

Nonlinear thermal effects play a critical role in enhancing the mechanical and electromagnetic performance of FG nanobeams. The stable amplitude response under varying electric voltages suggests that the material can maintain consistent performance despite changes in electrical input, which is essential for applications requiring precise control. Fig. 8 demonstrates the variation of the amplitude versus dimensionless frequency of the FG nanobeam. For an increasing dimensionless frequency, the amplitude shows linear growth in the curve until $\Omega = 1.9$, and afterwards, the curve reaches a rapid increment when electric voltage $V_0 = 1$. Likewise, when

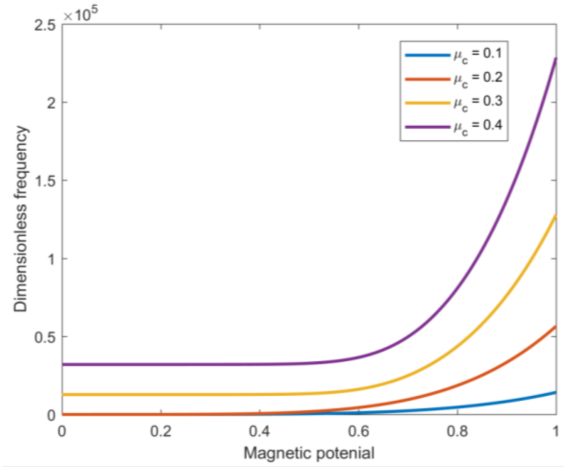

Fig. 4 The variation of frequency versus magnetic potential with the dominance of ceramic phase

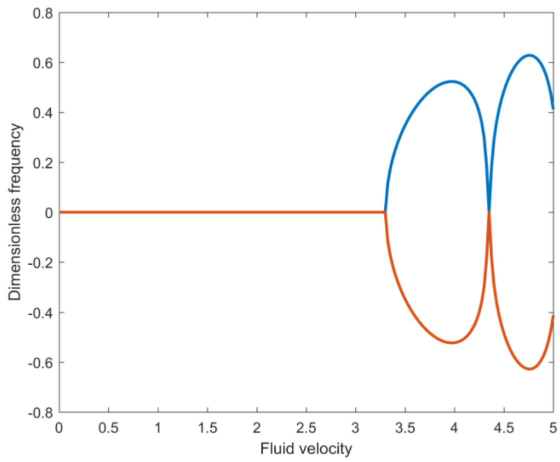

Fig. 5 Effect of dimensionless frequency over fluid velocity in the context of metal nonlocal variable

$V_0 = 0.5,1.5$, the dimensionless frequency reaches its maximum point of amplitude. Hence, at some watts of voltages, the amplitude-frequency relationship shows higher and lower modes eventually.

Considering Fig. 8, Fig. 9 shows an enlargement in amplitude axis from 0 to 2 with various electric voltages $V_0 = 0.5,1,1.5$ for the same amplitude-frequency relationship of nonlinear thermal FG nanobeams. In Fig. 10, the impact of variable nonlocal parameters μ_c, μ_m with magnetic field shows an ascending trend owing to its properties of ceramics and metals. Metals usually respond linearly to a magnetic field. Furthermore, the temperature increases with a rise in ceramic phase and decreases with the metal phase. Ceramics can show a range of magnetic and thermal responses based on their composition and structure. In Fig. 11, the impact of dimensionless frequency over piezoelectric strain and Young's modulus with different mode numbers is depicted. The 3D representation in Fig. 12 shows the changing behavior of temperature over the physical variables time and distance.

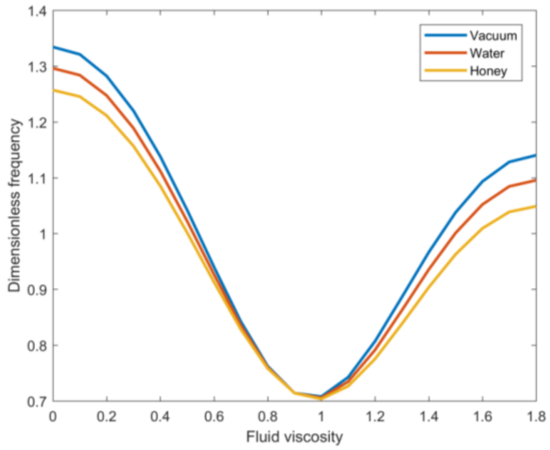

Fig. 6 Effect of dimensionless frequency on fluid viscosity with variants of viscous fluids in metal phase

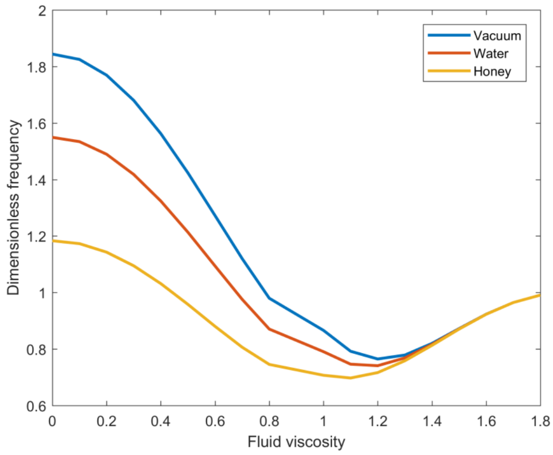

Fig. 7 Effect of dimensionless frequency on fluid viscosity with variants of viscous fluids in ceramic phase

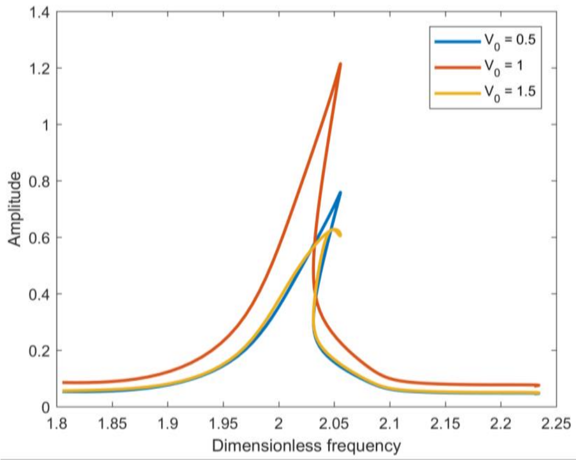

Fig. 8 The amplitude-frequency response of nonlinear thermal FG nanobeams with various electric voltages

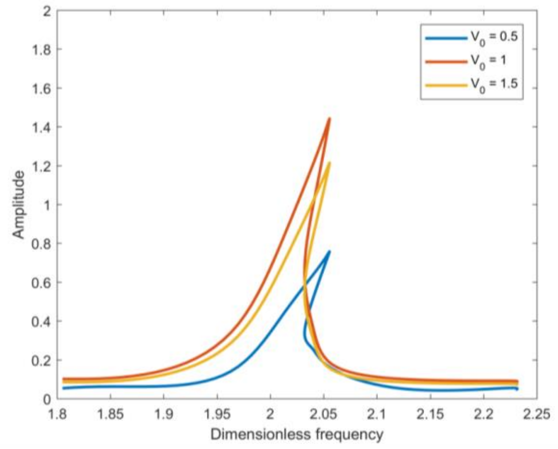

Fig. 9 The amplitude-frequency response of nonlinear thermal FG nanobeams with various electric voltages

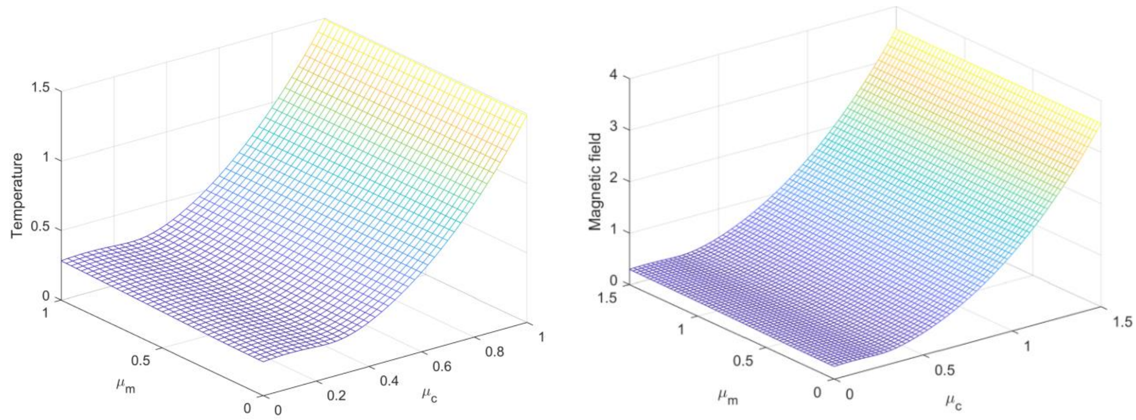

Fig. 10 Effect of variable nonlocal (μ_c, μ_m) over magnetic field and temperature

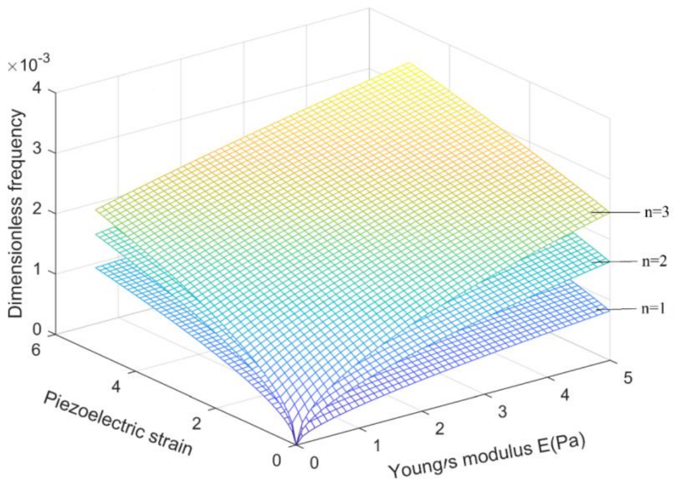

Fig. 11 A 3D plot shows the behavior of Young's modulus, Piezoelectric strain and Dimensionless frequency

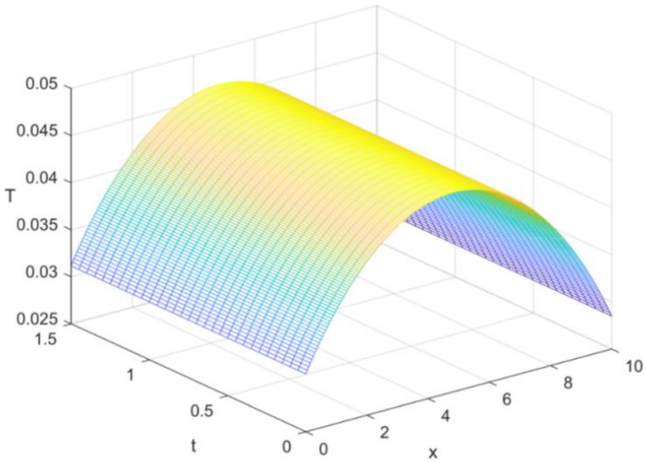

Fig. 12 A 3D plot shows the impact of time and distance on temperature

6. Conclusions

The study presented above focuses on the free vibration analysis of a fluid infiltrated porous nanobeam made of Functionally Graded Materials (FGM). To acquire the motion equations of the FG nanobeam, Hamilton's principle was employed. The derivation of the governing equations was achieved by inserting the displacement field equations into the Euler-Lagrange equations of the beam. These equations were then formulated as symmetric matrices using Navier's Solution method to obtain the necessary solutions. The significant outcomes of this research are highlighted as follows:

• Materials with stronger nonlocal effects has more pronounced decrease in temperature gradient as the imperfection ratio increases.

• The impact of variable nonlocal parameters with magnetic field shows an ascending trend owing to its properties of ceramics and metals.

• The imperfection ratio decreases with developing nonlocal material constants.

• Higher fluid viscosity, which in turn decreases the dimensionless frequency whereas, higher fluid velocity makes a resonant behavior with dimensionless frequency.

• For higher electric voltages, there will be larger the deformations or displacements which results in larger amplitudes.

• Nonlinear thermal effects significantly impact mechanical and electromagnetic performance of FG nanobeam, as evidenced by the stable amplitude with varying electric voltages and the ascending trend with variable nonlocal parameters in a magnetic field.

The study's findings can serve as benchmark results for future research, particularly in the dynamic analysis of nanostructures incorporating variable small-scale parameters along with electromagneto-thermal effects.

References

Alghamdi, N.A. (2024), "Coupled influences of magnetic field and several thermal loads on vibration of thermoelastic nano-ceramic (Si3N4) beam", *J. Eng. Res*., https://doi.org/10.1016/j.jer.2024.02.014.

Alibeigi, B., Tadi Beni, Y. and Mehralian, F. (2018), "On the thermal buckling of magneto-electro-elastic piezoelectric nanobeams", *Eur. Phys. J. Plus*, **133**, 1-18. https://doi.org/10.1140/epjp/i2018-11954-7.

Alibeigi, B., Tadi Beni, Y. and Mehralian, F. (2018), "On the thermal buckling of magneto-electro-elastic piezoelectric nanobeams", *Eur. Phys. J. Plus*, **133**, 1-18. https://doi.org/10.1140/epjp/i2018-11954-7.

Arefi, M. and Zenkour, A.M. (2017), "Wave propagation analysis of a functionally graded magneto-electro-elastic nanobeam rest on Visco-Pasternak foundation", *Mech. Res. Commun.*, **79**, 51-62. https://doi.org/10.1016/j.mechrescom.2017.01.004.

Arshid, E., Ghorbani, M.A., Momeni Nia, M.J., Civalek, Ö. and Kumar, A. (2023) "Thermo-elastic buckling behaviors of advanced fluid-infiltrated porous shells integrated with GPLs-reinforced nanocomposite patches", *Mech. Adv. Mater. Struct.*, 1-17. https://doi.org/10.1080/15376494.2023.2251015.

Barretta, R., Fabbrocino, F. and Luciano, R. (2018), "Closed-form solutions in stress-driven two-phase integral elasticity for bending of functionally graded nano-beams", *Physica E: Low Dimens. Syst. Nanostruct.*, **97**, 13-30. https://doi.org/10.1016/j.physe.2017.09.026.

Beni, Y.T. (2022), "Size dependent coupled electromechanical torsional analysis of porous FG flexoelectric micro/nanotubes", *Mech. Syst. Signal Pr.*, **178**, 109281. https://doi.org/10.1016/j.ymssp.2022.109281.

Beni, Y.T. (2023), "Size-dependent electro-thermal buckling analysis of flexoelectric microbeams", *Int. J. Struct. Stab. Dyn.*, **24**(08), 2450093. https://doi.org/10.1142/S0219455424500937.

Beni, Z.T. and Beni, Y.T. (2022), "Dynamic stability analysis of size-dependent viscoelastic/piezoelectric nano-beam", *Int. J. Struct. Stab. Dyn.*, **22**(05), 2250050. https://doi.org/10.1142/S021945542250050X.

Ebrahimi, F. (2021), "Wave dispersion in viscoelastic FG nanobeam via a novel spatial - temporal nonlocal strain gradient framework", *Wave. Random Complex Media*, 1-23. https://doi.org/10.1080/17455030.2021.1970282.

Ebrahimi, F. and Barati, M.R. (2017), "Size-dependent vibration analysis of viscoelastic nanocrystalline silicon nanobeams with porosities based on a higher order refined beam theory", *Compos. Struct*., **166**, 256-267. https://doi.org/10.1016/j.compstruct.2017.01.036.

Ebrahimi, F. and Barati, M.R. (2018), "Vibration analysis of smart piezoelectrically actuated nanobeams subjected to magneto-electrical field in thermal environment", *J. Vib. Control*, **24**, 549-564. https://doi.org/10.1177/1077546316646239.

Ebrahimi, F. and Barati, M.R. (2018), "Vibration analysis of smart piezoelectrically actuated nanobeams subjected to magneto-electrical field in thermal environment", *J. Vib. Control*, **24**, 549-564. https://doi.org/10.1177/1077546316646239.

Ebrahimi, F. and Dabbagh, A. (2017), "Wave propagation analysis of embedded nanoplates based on a nonlocal strain gradient-based surface piezoelectricity theory", *Eur. Phys. J. Plus*, **132**, 449. https://doi.org/10.1140/epjp/i2017-11694-2.

Ebrahimi, F. and Jafari, A. (2016), "A higher-order thermomechanical vibration analysis of temperature-dependent FGM beams with porosities", *J. Eng.*, **2016**(1), 9561504. https://doi.org/10.1155/2016/9561504.

Ebrahimi, F. and Salari, E. (2016), "Effect of various thermal loadings on buckling and vibrational characteristics of nonlocal temperature-dependent functionally graded nanobeams", *Mech. Adv. Mater. Struct.*, **23**,1379-1397. https://doi.org/10.1080/15376494.2015.1091524.

Ebrahimi, F., Jafari, A. and Selvamani, R. (2020), "Thermal buckling analysis of magneto-electro-elastic porous FG beam in thermal environment", *Adv. Nano Res.*, **8**(1) 83.

Ebrahimi, F., Karimiasl, M. and Selvamani, R. (2020), "Bending analysis of magneto-electro piezoelectric nanobeams system under hygro-thermal loading", *Adv. Nano Res*., **8**, 203-214. https://doi.org/10.12989/anr.2020.8.3.203.

Ebrahimi, F., Karimiasl, M. and Singhal, A. (2021), "Magneto-electro-elastic analysis of piezoelectric-flexoelectric nanobeams rested on silica aerogel foundation", *Eng. Comput*., **37**, 1007-1014. https://doi.org/10.1007/s00366-019-00869-z.

Ghobadi, A., Beni, Y.T. and Golestanian, H. (2020), "Nonlinear thermo-electromechanical vibration analysis of size-dependent functionally graded flexoelectric nano-plate exposed magnetic field", *Arch.*

Appl. Mech., **90**, 2025-2070. https://doi.org/10.1007/s00419-020-01708-0.
Hosseini, S.M.H. and Beni, Y.T. (2023), "Free vibration analysis of rotating piezoelectric/flexoelectric microbeams", *Appl. Phys. A*, **129**(5), 330. https://doi.org/10.1007/s00339-023-06615-z.
Jena, S.K., Chakraverty, S. and Malikan, M. (2020), "Stability analysis of nanobeams in hygrothermal environment based on a nonlocal strain gradient Timoshenko beam model under nonlinear thermal field", *J. Comput. Des. Eng.*, **7**(6), 685-699. https://doi.org/10.1093/jcde/qwaa051
Ke, L.L. and Wang, Y. (2014), "Free vibration of size-dependent magneto-electro-elastic nanobeams based on the nonlocal theory", *Physica E: Low Dimens. Syst. Nanostruct.*, **63**, 52-61. https://doi.org/10.1016/j.physe.2014.05.002.
Ke, L.L. and Wang, Y.S. (2012), "Thermoelectric-mechanical vibration of piezoelectric nanobeams based on the nonlocal theory", *Smart Mater. Struct.*, **21**, 025018. https://doi.org/10.1088/0964-1726/21/2/025018.
Ke, L.L., Wang, Y.S. and Wang, Z.D. (2012), "Nonlinear vibration of piezoelectric based on the nonlocal theory", *Compos. Struct.*, **94**, 2038-2047. https://doi.org/10.1016/j.compstruct.2012.01.023.
Kiani, Y. and Eslami, M.R. (2010), "Thermal buckling analysis of functionally graded material beams", *Int. J. Mech. Mater. Des.*, **6**, 229-238. https://doi.org/10.1007/s10999-010-9132-4.
Li, L. and Hu, Y. (2016), "Nonlinear and free vibration analysis of nonlocal strain gradient beams made of functionally graded material", *Int. J. Eng. Sci.*, **102**, 77-92. https://doi.org/10.1016/j.ijengsci.2016.07.011.
Li, S.R., Su, H.D. and Cheng, C.J. (2009), "Free vibration of functionally graded material beams with surface-bonded piezoelectric layers in thermal environment", *Appl. Math. Mech.*, **30**, 969-982. https://doi.org/10.1007/s10483-009-0803-7.
Lim, C.W., Zhang, G. and Reddy, J. (2015), "A higher-order nonlocal elasticity and strain gradient theory and its applications in wave propagation", *J. Mech. Phys. Solid.*, **78**, 298-313. https://doi.org/10.1016/j.jmps.2015.02.001.
Mirjavadi, S.S., Yahya, Y.Z., Forsat, M., Khan, I., Hamouda, A.M.S. and Barati, M.R. (2020), "Magneto-electric effects on nonlocal nonlinear dynamic characteristics of imperfect multi-phase magneto-electro-elastic beams", *J. Magnet. Magnet. Mater.*, **503**, 166649. https://doi.org/10.1016/j.jmmm.2020.166649.
Nguyen, T.K., Nguyen, T.T.P., Vo, T.P. and Thai, H.T. (2015), "Vibration and buckling analysis of functionally graded sandwich beams by a new higher-order shear deformation theory", *Compos. Part B: Eng.*, **76**, 273-285. https://doi.org/10.1016/j.compositesb.2015.02.032.
Rad, E.S., Saidi, A.R., Rezaei, A.S. and Askari, M. (2020), "Shear deformation theories for elastic buckling of fluid-infiltrated porous plates: An analytical approach", *Compos. Struct.*, **254**, 112829. https://doi.org/10.1016/j.compstruct.2020.112829.
Reddy, J.N. and El-Borgi, S. (2014), "Eringen's nonlocal theories of beams accounting for moderate rotations", *Int. J. Eng. Sci.*, **82**, 159-177. https://doi.org/10.1016/j.ijengsci.2014.05.006.
Romano, G. and Barretta, R. (2017), "Stress-driven versus strain-driven nonlocal integral model for elastic nano-beams", *Compos. Part B: Eng.*, **114**, 184-188. https://doi.org/10.1016/j.compositesb.2017.01.008.
Selvamani, R., Loganathan, R., Dimitri, R. and Tornabene, F. (2023), "Nonlocal state-space strain gradient wave propagation of magneto thermo piezoelectric functionally graded nanobeam", *Curv. Layer. Struct.*, **10**(1), 20220192. https://doi.org/10.1515/cls-2022-0192.
Shariati, A., Ebrahimi, F. and Karimiasl, M. (2020), "On bending characteristics of smart magneto-electro-piezoelectric nanobeams system", *Adv. Nano Res.*, **9**, 183-191. https://doi.org/10.12989/anr.2020.9.3.183.
Sun, D. and Luo, S.N. (2011), "Wave propagation of functionally graded material plates in thermal environments", *Ultrasonic.*, **51**, 940-952. https://doi.org/10.1016/j.ultras.2011.05.009.
Thai, H.T. and Choi, D.H. (2012), "A refined shear deformation theory for free vibration of functionally graded plates on elastic foundation", *Compos. Part B*, **43**, 2335-2347. https://doi.org/10.1016/j.compositesb.2011.11.062.
Thai, H.T., Park, T. and Choi, D.H. (2013), "An efficient shear deformation theory for vibration of functionally graded plates", *Arch. Appl. Mech.*, **83**, 137-149. https://doi.org/10.1007/s00419-012-0642-4.
Van Vinh, P. and Tounsi, A. (2022), "The role of spatial vibration of the nonlocal parameter on the free vibration of functionally graded sandwich nanoplates", *Eng. Comput.*, **38**(Suppl 5), 4301-4319.

https://doi.org/10.1007/s00366-021-01475-8.

Xiao, W.S., Gao, Y. and Zhu, H. (2019), "Buckling and post-buckling of magneto-electro-thermo-elastic functionally graded porous nanobeams", *Microsyst. Technol.*, **25**, 2451-2470. https://doi.org/10.1007/s00542-018-4145-2.

CC